Available at www.sciencedirect.com

ScienceDirect

journal homepage: www.elsevier.com/locate/watres

Development of a TiO_2 modified optical fiber electrode and its incorporation into a photoelectrochemical reactor for wastewater treatment

K. Esquivel[a], L.G. Arriaga[a], F.J. Rodríguez[a], L. Martínez[b], Luis A. Godínez[a,*]

[a]Centro de Investigación y Desarrollo Tecnológico en Electroquímica, Electrochemistry Department, S.C. Parque, Tecnológico Querétaro Sanfandila, Pedro Escobedo 76703, Querétaro, México

[b]Instituto de Investigaciones Científicas, Universidad de Guanajuato, Guanajuato, México

ARTICLE INFO

Article history:
Received 8 January 2009
Received in revised form
6 May 2009
Accepted 6 May 2009
Published online 6 June 2009

Keywords:
TiO_2 optical fiber electrode
TiO_2
Azo orange II
Electrochemical advanced oxidation processes (EAOPs)

ABSTRACT

Electrochemical advanced oxidation processes (EAOPs) are used to chemically burn non biodegradable complex organic compounds that are present in polluted effluents. A common approach involves the use of TiO_2 semiconductor substrates as either photocatalytic or photoelectrocatalytic materials in reactors that produce a powerful oxidant (hydroxyl radical) that reacts with pollutant species. In this context, the purpose of this work is to develop a new TiO_2 based photoanode using an optic fiber support. The novel arrangement of a TiO_2 layer positioned on top of a surface modified optical fiber substrate, allowed the construction of a photoelectrochemical reactor that works on the basis of an internally illuminated approach. In this way, a semi-conductive optical fiber modified surface was prepared using 30 μm thickness SnO_2:Sb films on which the photoactive TiO_2 layer was electrophoretically deposited. UV light transmission experiments were conducted to evaluate the transmittance along the optical fiber covered with SnO_2:Sb and TiO_2 showing that 43% of UV light reached the optical fiber tip. With different illumination configurations (external or internal), it was possible to get an increase in the amount of photo-generated H_2O_2 close to 50% as compared to different types of TiO_2 films. Finally, the electro-Fenton photoelectrocatalytic Oxidation process studied in this work was able to achieve total color removal of Azo orange II dye (15 mg L^{-1}) and a 57% removal of total organic carbon (TOC) within 60 min of degradation time.

1. Introduction

Advanced oxidation processes (AOPs) have been identified as a successful alternative for the elimination of some toxic organic compounds in water. These processes are chemical, photochemical, photocatalytic or electrochemical methods characterized by the generation of the hydroxyl radical species ($OH^{\bullet}$) (Yu et al., 2008; Tomovska et al., 2007; Lou and Huang, 2008; Lapertot et al., 2008; Bandala et al., 2008; Orozco et al., 2008; Guinea et al., 2008). The hydroxyl radical is a strong oxidant with a standard potential of 2.8 V vs NHE (pH 0) capable of destroying most of the organic matter present in water.

Recently, there has been an increasing interest in the use of the so-called Electrochemical Advanced Oxidation Processes (EAOPs) (Martínez-Huitle and Brillas, 2009; Skoumal et al.,

* *Corresponding author*. Tel.: +52 442 2116006; fax: +52 442 2116007.
E-mail address: lgodinez@cideteq.mx (L.A. Godínez).
URL: http://www.cideteq.mx

0043-1354/$ – see front matter © 2009 Elsevier Ltd. All rights reserved.
doi:10.1016/j.watres.2009.05.035

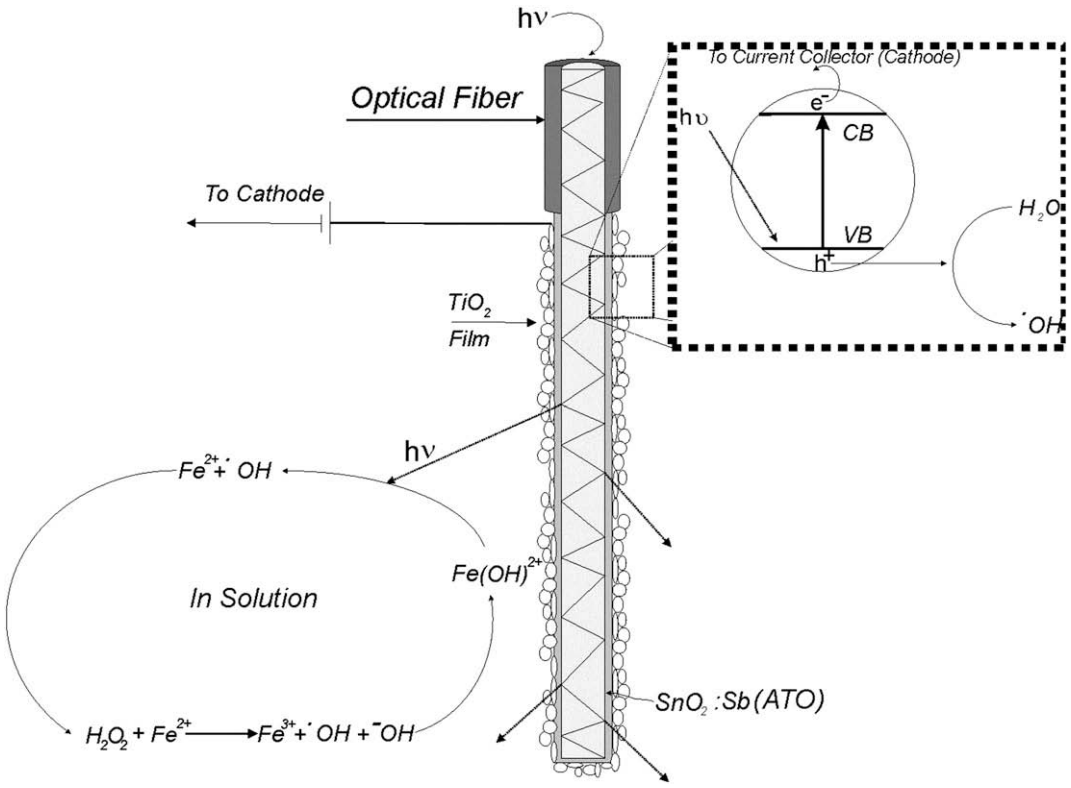

Fig. 1 – Scheme of the novel TiO_2 modified optical fiber electrode.

2009; Wang et al., 2009; Bandara et al., 2007) which consist on electrochemical methods that result in the generation of hydroxyl radicals (OH•) or its precursor, hydrogen peroxide. In this way, while the OH• radical can be directly generated on the surface of an anode M (see Eq. (1)), its production can be achieved indirectly by generation of H_2O_2 (through the reduction of dissolved oxygen in water under slightly acidic conditions according to Eq. (2) (Brillas et al., 2003; Boye et al., 2003))

$$M + H_2O \rightarrow M(OH^{\bullet}) + H^+ + e^- \quad (1)$$

$$O_{2(g)} + 2H^+ + 2e^- \rightarrow H_2O_2 \quad (2)$$

Hydrogen Peroxide, as can be seen in Eq. (3), can react with Fe^{2+} ions (pH 2–3) to produce OH• radicals in an arrangement known as the Electro-Fenton process (Peralta-Hernández et al., 2007; Özcan et al., 2009; Virkutyte and Jegatheesan, 2009; Serra et al., 2008).

$$H_2O_2 + Fe^{2+} \rightarrow Fe^{3+} + OH^- + OH^{\bullet} \quad (3)$$

Reaction 3 is propagated by Fe^{2+} regeneration, resulting from reduction of Fe^{3+} at the cathode (Flox et al., 2007a, b; Oturan et al., 2008).

A feasible alternative is the use of the photoelectro-Fenton process where the application of UV light promotes the photodecomposition of complexes of Fe^{3+} with generated carboxylic acids (Boye et al., 2002; Sirés et al., 2006) and the regeneration of Fe^{2+} from photoreduction of $Fe(OH)^{2+}$, which is the predominant form of the Fe^{3+} species in aqueous solution (Eq. (4)):

$$Fe(OH)^{2+} + h\upsilon \rightarrow Fe^{2+} + OH^{\bullet} \quad (4)$$

Advanced oxidation technology studies often have included semiconductor photocatalyst as well and in this regard, titanium dioxide (TiO_2) has been proven to be an effective catalyst for oxidation and mineralization of organic pollutants (Wang et al., 2007). Previous works in our research group (Peralta-Hernández et al., 2007, 2008) as well as in others (Li et al., 2006; Jiang et al., 2006; Zhao et al., 2007) have focussed on the use of TiO_2 electrodes showing that it can be efficiently used as anodes in a photoelectrochemical reactor. The use of the TiO_2 in this approach involves the light induced promotion of an electron (e^-) from the valence band (VB) into the conduction band (CB), thus creating a hole (h^+) in the later according to Eq. (5) (Gumy et al., 2008; Fujishima et al., 2000). The e^-/h^+ pair can be separated under the influence of an applied potential forcing the electron to travel trough the electric circuit towards the cathode favoring at the same time, the reaction of the positively charged vacancy, h^+, with either adsorbed water or hydroxyl ions to produce the powerful OH• oxidant (Eqs. (6) and (7)).

$$TiO_2 + h\upsilon \rightarrow e^-_{CB} + h^+_{VB} \quad (5)$$

$$h^+_{vb} + H_2O \rightarrow OH^{\bullet} + H^+ \quad (6)$$

$$h^+_{vb} + OH^- \rightarrow OH^{\bullet} \quad (7)$$

The effectiveness of the oxidation process can also be enhanced through the direct oxidation of the organic compound, R, by the positively charged vacancy (h^+_{vb}, Eq. (8))

$$h^{+}_{vb} + R \rightarrow R^{+}_{ox} \quad (8)$$

Under typical conditions however, illumination of the semiconductor electrode in these reactors is not optimized due to the absorption and scattering of the radiation by the reaction medium (Danion et al., 2004a, b, 2006, 2007). As proposed and theoretically evaluated by Marinangeli and Ollis (1977, 1980, 1982), a feasible solution for this problem is the use of an optical fiber as a light distributor and support of the photocatalyst. Several works have developed, characterized, and modelled an optical fiber reactor (OFR) system for water treatment (Peill and Hoffmann, 1998; Choi et al., 2001; Wang and Ku, 2003) and others have demonstrated that the covered optical fiber with TiO_2 films can be used for the photocatalytic oxidation of organic compounds (Miller et al., 1999).

So far however, the use of a TiO_2 modified optical fiber as *photoanode* in a photoelectrochemical wastewater treatment reactor has not been published. Therefore, in this work we report the construction of an optical fiber-based electrode covered with TiO_2 and its use for the oxidation of the model textile dye Orange II.

Since the optical fiber carries light along its length and is made from a nonconducting material (SiO_2), it was necessary to previously modify the fiber by promoting holes or cracks along its surface (so that light could escape) and later, deposit a semiconductor material (SnO_2:Sb) on which the formation of the photocatalytically active TiO_2 film could be carried out by electrophoretic deposition (see Fig. 1). As a part of this work, we evaluated the physicochemical characteristics of the SnO_2:Sb and TiO_2 films and the influence of the coating thickness and fiber length on the light transmission and on the photocatalytic production of H_2O_2.

2. Materials and methods

2.1. Optical fiber treatment

Optical fiber O.F. P600-12-UV/VIS (Ocean Optics, USA) with a 600 μm silica core and a polymer optical cladding was used. Each optical fiber was cut into pieces of 20 cm in length and 10 cm of optical cladding was removed by heating at 500 °C. Fiber ends were polished with abrasive paper. The fibers were pre-treated with HF (48–51%, J.T. Baker) solution and later rinsed with deionized water. Scanning electron microscopy (SEM) and emission diffraction X-ray (EDX) analysis were completed using a JEOL JSM-5400L microscope with an accelerating voltage of 25 kV.

2.2. Antimony tin oxide (SnO_2:Sb) film

These films were prepared on top of the pre-treated optical fiber material to provide a rough and conducting surface on which the TiO_2 films could later be grown by electrophoretic deposition. The ATO (Antimony Tin Oxide) material was chosen for its conductive properties and for its optical transparency in the visible spectral region. The films were prepared using the painting technique. The solution was prepared using 11 g of $SnCl_4$ (98% Strem Chemicals) dissolved in 5 mL hydrochloric acid (HCl, 36.5–38.0% J.T. Baker) and heated at 90 °C for 30 min. Afterwards, 10 mL of methanol were added to the $SnCl_4$ solution in order to prepare the starting mixture. Finally, to prepare the doped solution, $SbCl_3$,(99% Strem Chemicals) was dissolved in 2-propanol (2-Propanol 99.97% J.T. Baker) and added to the starting solution to form a 2 % w/w solution (Elangovan and Ramamurthi, 2003).

The SnO_2:Sb films were heated at 450 °C for 10 min in a tubular furnace (Thermoline model 21100) in order to promote the formation of the oxidized species of tin and antimony (SnO_2, Sb_2O_3 and Sb_2O_5). The SnO_2:Sb films were characterized by SEM, EDX, X-ray diffraction (XRD), light transmission and perfilometry.

2.3. TiO_2 film

TiO_2 films were deposited on the pre-treated fibers using the electrophoretic deposition method in which the fiber was immersed for 60 s at room temperature in a sonicated 250 mL colloidal suspension (12.5 gr P25 Degussa TiO_2 powder in 5% v/v 2-propanol, J.T. Baker 99.97% in deionized water) under a 4 V potential difference applied between a stainless steel sheet and the optical fiber previously coated with SnO_2:Sb. The electrodes were then placed in an oven at 450 °C to sinter the TiO_2 film (Manriquez and Godínez, 2007).

2.4. Light transmission across the SnO_2:Sb–TiO_2 films

The measurement of light transmitted by the coated fiber was made with a light sensitive photo-resistance semiconductor (CdS) with a maximum detection limit of 15 MΩ. The photo-resistance semiconductor was connected to a multimeter (Fluke Model 45) to measure the electrical resistance. The fraction of light transmitted, I_{trans}/I_{input}, was obtained by calculating the ratio of the electrical resistance between the value obtained placing the resistance at the specific point of analysis, R_{trans}, and the value obtained at the illumination source, R_0,(Eq. (9), Pallas, 2005). All the measurements were performed in a darkroom.

$$\frac{I_{trans}}{I_{input}} = \frac{R_{trans}}{R_0} \quad (9)$$

2.5. H_2O_2 photocatalytic generation

To measure the influence of the illumination arrangement mode (internal or external) and the effect of the number of TiO_2 layers deposited on the light conducting substrate on the production of hydrogen peroxide, a bundle of 25 fibers was placed in a 0.05 M Na_2SO_4 (Karal, 7039) solution at pH 3 (adjusted with sulfuric acid, 98%, J.T. Baker) previously saturated with oxygen (O_2 99.99%, Infra). For externally illuminated photocatalysis experiments, the bundle was irradiated using a low pressure UV mercury lamp ($\lambda = 254$ nm, $P = 21$ W cm^{-2}. UVP, Inc.) for 60 min. The H_2O_2 generated was determined by the titanium (IV) oxysulfate method ($TiOSO_4$, 99.99%, ca. 15 wt. diluted sulfuric acid solution ALDRICH) that is based on the color intensity measurement of the H_2O_2–reagent complex at 406 nm (Brillas et al., 2003). In order to compare the performance of the electrode for H_2O_2 production using an internal illumination arrangement mode, the same electrode was illuminated from one end of the fiber bundle

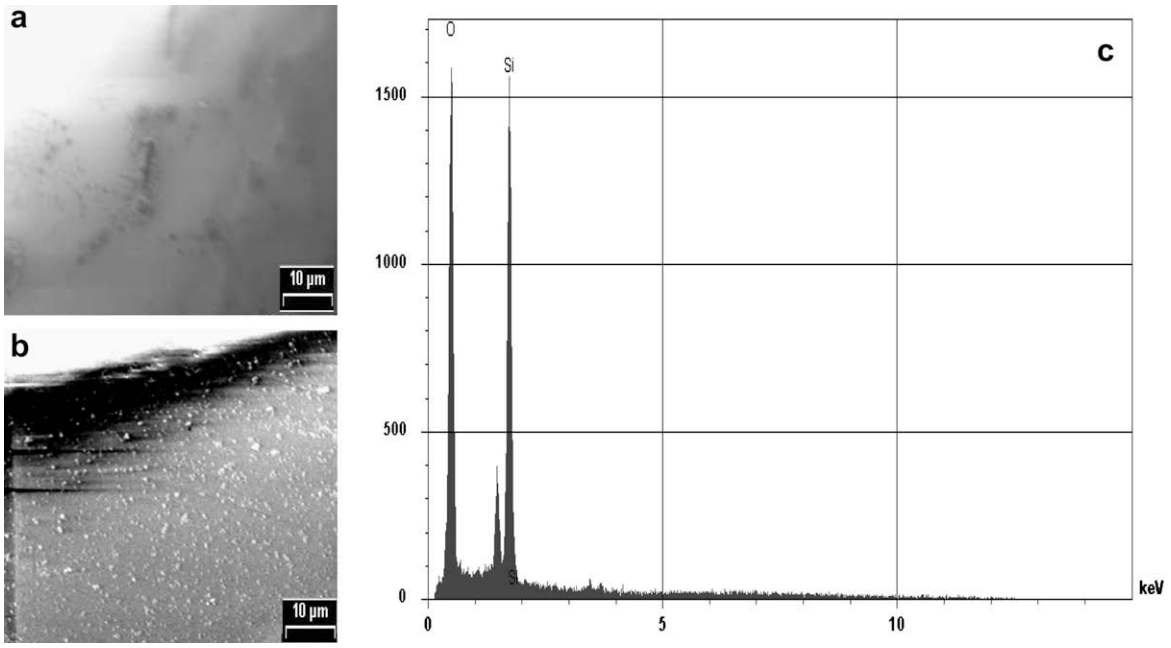

Fig. 2 – SEM images of the surface of an optical fiber (a) before and (b) after HF treatment. (c) Corresponds to the EDX spectra of the optical fiber surface after HF treatment.

using the same lamp under similar experimental conditions. The hydrogen peroxide production was also measured using the titanium (IV) oxysulfate method.

2.6. *Electrochemical generation of H_2O_2*

Hydrogen peroxide was simultaneously produced at the cathode and the anode in an electrochemical arrangement. In the former electrode, it was produced by the electrochemical reduction of the dissolved oxygen on a carbon cloth cathode (ElectroChem, Inc.) characterized by 69 cm^2 of geometric area (Eq. (2)). In the anodic side, a bundle of 25 optical fibers coated with SnO_2:Sb and TiO_2 (13 cm^2 geometric area) worked as an anode producing H_2O_2 trough the electrochemical oxidation of water. The electrolyte consisted of a sulphate buffer (Na_2SO_4) solution at pH 3. The experimental system included a fiberglass electrochemical reactor with three individual chambers of 9 cm length and 5.5 cm inner diameter. The reactor volume was 640 mL and the recirculation flow rate was maintained at 80 L h^{-1} using a diaphragm pump (Shurflo Model 2088-594-154). The experiments were performed under galvanostatic conditions applying 1 mA cm^{-2} cathodic current density using a GW Model GPR-1820HD power supply.

2.7. *Electrochemical advanced oxidation processes (EAOPs)*

Four different processes were evaluated by measuring the color removal of a 15 mg L^{-1} Orange II ($C_{16}H_{11}N_2NaO_4S$, ALDRICH) solution using the electrochemical reactor:

(i) Anodic electrooxidation; which consists on electron transfer from the dye molecule to the anode. In this case, hydroxyl radicals can also be produced from the Electrolytic-Oxidation of water on the anode surface (Eq. (1) (Xie and Li, 2006).

(ii) Electro-assisted photocatalytic oxidation; which is a process that involves the photocatalytic oxidation reaction of the dye on a polarized photo excited TiO_2 electrode. While the applied potential favors charge carrier separation (Selcuk et al., 2004; Wang et al., 2008; Neelavannan and Basha, 2008; Hou et al., 2009; Yang et al., 2009), UV illumination of the anodic material (Eqs. (5)–(8)) was conducted under internal and external arrangement modes.

(iii) Electro-Fenton; that combines the reactions that occur in the Fenton system (Eq. (3)) and those described in (i).

(iv) The electro-Fenton photoelectrocatalytic Oxidation process that considers the combination of the photoelectrocatalytic reactions of TiO_2 (ii) and the photoelectro-Fenton reactions shown in Eqs. (3) and (4) (Xie and Li, 2006).

The photo assisted processes were performed with the UV lamp used in the H_2O_2 generation studies. In the case of the electro-Fenton and electro-Fenton photoelectrocatalytic Oxidation processes, 0.2 mM of $FeSO_4$ was added as the Fe^{2+} ion source (98% J.T. Baker). The removal of color was evaluated by determining the absorbance of the solution at $\lambda = 487$ nm in a UV–vis spectrophotometer (Agilent Technologies). Total organic carbon (TOC) data was obtained using a TOC VSCN analyzer (Shimadzu Co.).

3. Results and discussion

3.1. *Optical fiber treatment*

Fig. 2 shows the SEM image of the optical fiber without the cladding (2a) and after it was pre-treated with HF (2b). As can

be observed, the morphology changed due to the formation of pores over the surface of the optical fiber. The EDX test indicated the presence of Si and O_2 and the absence of F, so pore formation was only due to chemical attack by HF as no other species were found on the surface (Fig. 2c). It is important to note that while the pre-treatment of the fiber was carried out to produce a light escaping path on the fiber surface (see Fig. 1), it also resulted in a rough surface on which adherence of the SnO_2:Sb and TiO_2 films could be favored.

3.2. *Antimony tin oxide (SnO_2:Sb) film*

A homogeneous deposit of tin oxide doped with antimony was obtained after repeating 10 times the painting process described in the experimental section (SEM images not shown). Although the electrical resistance of the SnO_2:Sb film was high (0.1 MΩ), a more aggressive thermal treatment to increase the conductivity was not tried since the optical transparency of the film could be affected (Russo and Cao, 2008). Despite the fact that the conductivity obtained with these films was relatively low, the adherence of the TiO_2 films that were later grown by electrophoretic deposition was favored by the presence of the transparent SnO_2:Sb film. The XRD patterns obtained from the SnO_2:Sb deposits on the other hand indicated the presence of tin and antimony oxides (Sb_2O_5 and Sb_2O_3). The profilometer experiments indicated that the thickness of the deposit is about 30 μm.

UV light transmission along the optical fiber was determined as received without the cladding and using the fiber treated with HF. The measurements were made with various lengths of the optical fiber. When a complete fiber was used, a loss of almost 30% of the UV radiation was measured in the first 10 cm due to refraction and reflection phenomena (Fig. 3a,(-■-)). When the polymer optical cladding was removed and the core was exposed, the UV light transmittance decreased to 45% in the first 2 cm of the fiber caused by the abrupt change of the refraction index between the SiO_2 and air (($n = 1.5$ vs $n = 1$) (-○-) (Wang and Ku, 2003)). The UV light transmittance in the HF treated fiber (-△-) decreased to 5% in the first 2 cm of the fiber.

The measurement of the UV light transmittance along the SnO_2:Sb covered fiber as a function of the number of deposits shows that 20 % of the UV light is absorbed or refracted by the chemical and structural properties of SnO_2:Sb films (Fig. 3b), and this percentage remains constant for the various numbers of films. According to these results, the thickness of the SnO_2:Sb does not affect the absorbance percentage, so the number of deposits do not limit the transmittance of the fiber.

3.3. *TiO_2 coating*

To reduce the electrical resistance in the SnO_2:Sb film in order to be able to carry out the electrophoretic deposition of TiO_2, carbon cloth threads were placed around the optical fiber already covered with SnO_2:Sb; thus obtaining an electrical resistance of the optical fiber surface of 50 Ω. Fig. 4 shows SEM images of the TiO_2 films deposited on the carbon cloth thread and on the optical fiber after two electrophoretic deposition layers were carried out. Under these conditions, the TiO_2 films

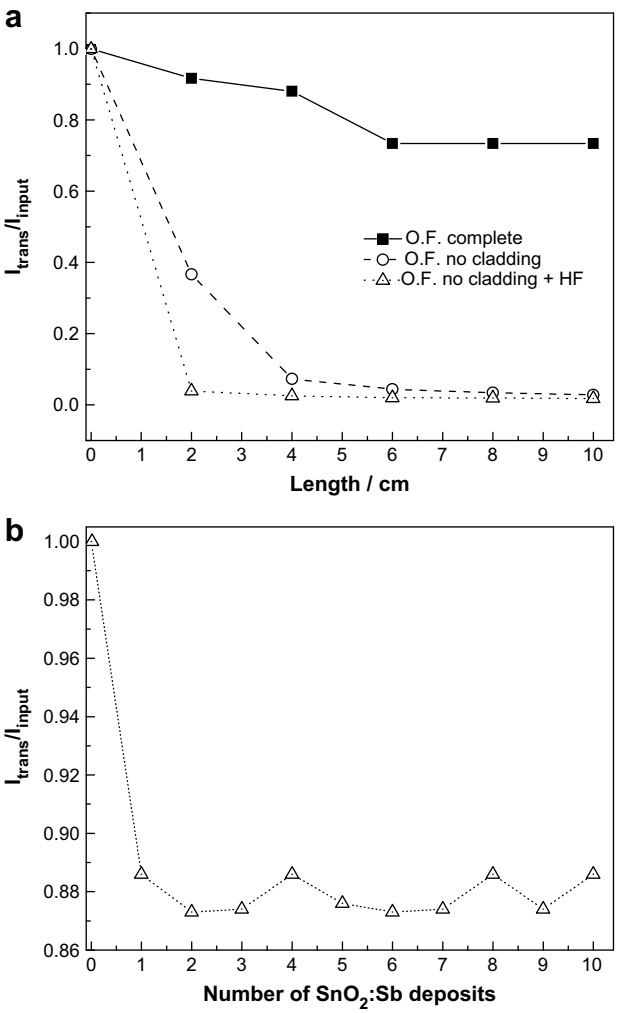

Fig. 3 – UV light transmission ratio of surface modified optical fibers as a function of (a) the fiber length, complete optical fiber (-■-), optical fiber without cladding (-○-), optical fiber without cladding and pre-treated (-△-) and (b) the number of SnO_2:Sb deposits.

have a homogenous and porous surface. However, when applying the deposition procedure from 3 to 10 times, the texture of the surface becomes compact and the deposits tend to crack and fall apart. The results obtained with the profilometer indicate that the thickness of the film ranged between 2.5 and 70 μm.

The transmittance in the optical fiber is affected by the thickness of the TiO_2 film that covers the external surface, so it was necessary to assess the effect of the TiO_2 deposit thickness on the global efficiency of light transmission. This effect was evaluated by measuring the light fed to the fiber (I_{input}) and the light transmitted throughout the optical fiber coated with TiO_2 (I_{trans}). According to the results obtained, the relationship I_{trans}/I_{input} decreases exponentially from 1.0 when there is no TiO_2, to 0.47 when the thickness of the TiO_2 film is 70 μm (Fig. 5).

The mathematical expression of Beer's law predicts that the fraction of refracted or absorbed light by the TiO_2 deposit

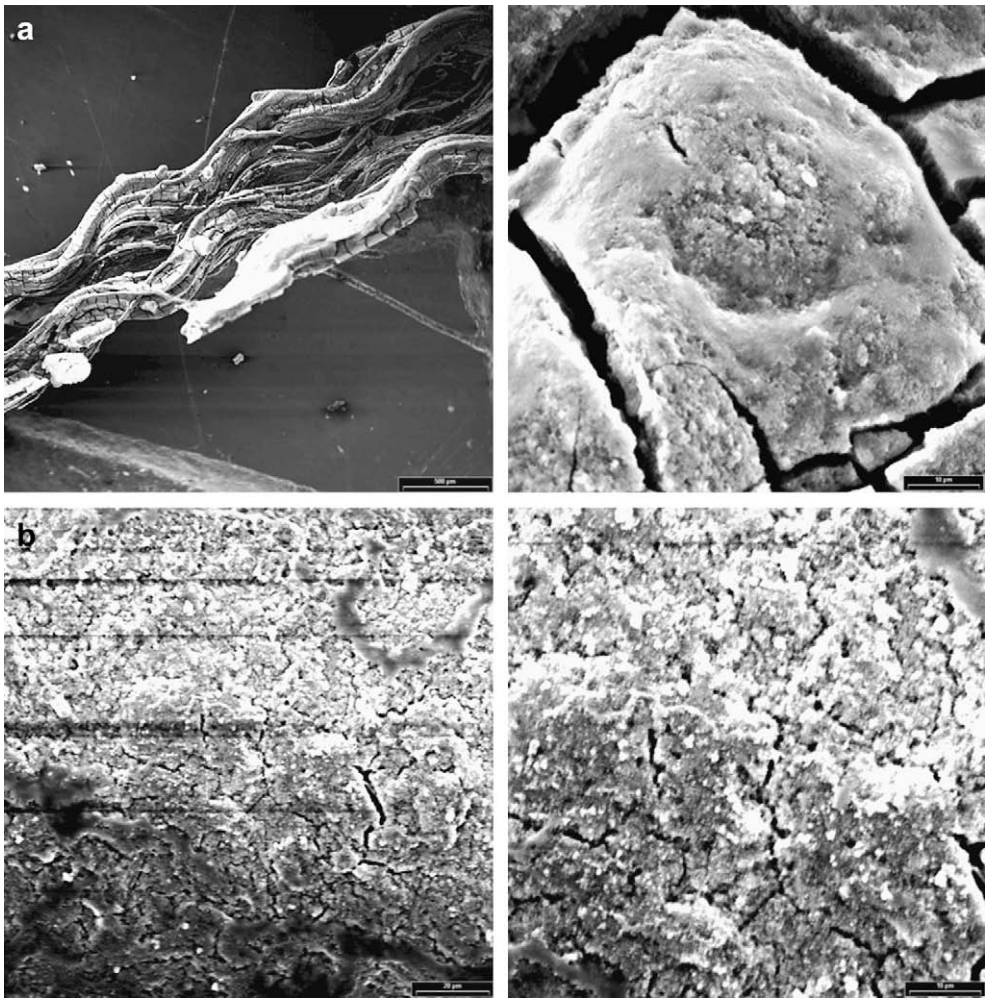

Fig. 4 – (a) SEM images of a TiO_2 film over carbon thread and (b) TiO_2 film over optical fiber.

should increase proportional to the increase of the deposit thickness. Choi et al. (2001) and Peill and Hoffmann (1995), adapted Beer's Law to the specific case of coated optical fibers:

$$\frac{I_{trans}}{I_{input}} = e^{-\varepsilon_{app}\delta} \tag{10}$$

$$\frac{I_{trans}}{I_{input}} = (1 - f_\theta) + f_\theta e^{-\varepsilon_{app}\delta} \tag{11}$$

where I_{input} is the input light intensity ($W\,cm^{-2}$); I_{trans} is the residual light intensity transmitted ($W\,cm^{-2}$); ε_{app} and δ are the apparent extinction coefficient and thickness of the coating respectively; f_θ is the fraction of incident light with $\theta < 90^\circ$ refracted and absorbed by the TiO_2 coating and $(1 - f_\theta)$ represents the fraction of near-parallel incident light that is not absorbed by the TiO_2 film.

The fitting of the experimental data to Eqs. (10) and (11) shows that the relationship I_{trans}/I_{input} decreases exponentially with the TiO_2 thickness and that the light transmitted through the semiconductor material reaches values near 0.5 for a TiO_2 thickness value of about 35 μm. The fitting of the data also allows the estimation of: 1) the fraction of near-parallel incident light $(1 - f_\theta)$ that is not absorbed by the TiO_2 coating (0.5261), 2) the fraction of incident light (f_θ) with $\theta < 90^\circ$ refracted and absorbed by the TiO_2 coating (0.4739) and 3) the value of the apparent extinction coefficient (ε_{app}) for the TiO_2 film (0.088 μm^{-1}).

3.4. *Photocatalytic generation of H_2O_2*

Once the TiO_2 modified optical fiber electrode was prepared and characterized, its performance as a photocatalytic material (under no polarization conditions) using UV radiation was tested. In these experiments, the difference between internal (light travelling and escaping along the optical fiber path, see Fig. 1) and external (from a source located outside the reaction cell) illumination modes on the TiO_2 modified fiber was evaluated by measuring the photocatalytic production of H_2O_2 in the presence of oxygen. Upon illumination of the TiO_2 modified substrate, hydrogen peroxide is assumed to be produced by reactions 5–7,12 and 13 (Bauer et al., 1999; Peralta-Hernández et al., 2006; Gianluca et al., 2008). This is supported

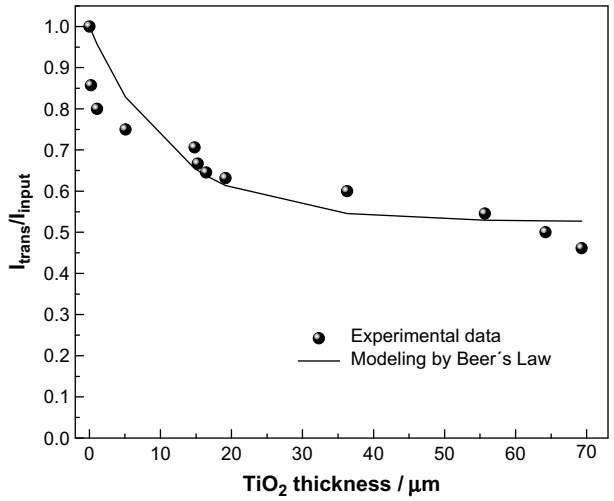

Fig. 5 – UV light transmission ratio (experimental and fitted data) of a TiO_2 modified optical fiber as a function of the coating thickness.

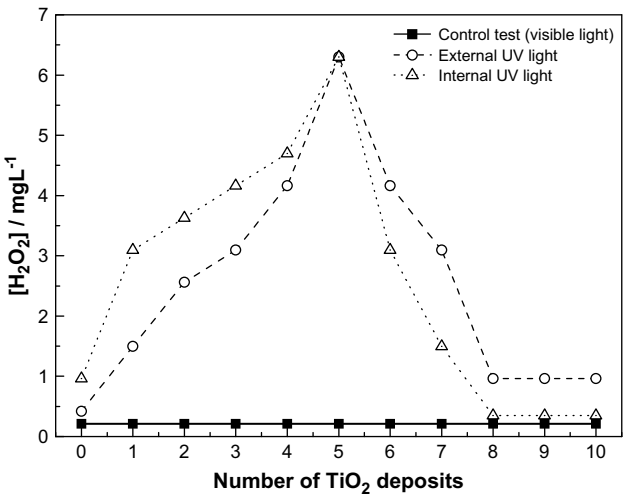

Fig. 6 – Photocatalytic production of H_2O_2 as a function of the number of deposits of TiO_2 on an optic fiber-based electrode under different illumination conditions, visible light (-■-), UV external illumination (-○-) and UV internal illumination (-△-). Illumination time, 60 min. Na_2SO_4 0.05 M pH 3 solution saturated with oxygen and without applied electric current.

by the data presented in Fig. 6 in which a control experiment without UV radiation does not result in H_2O_2 generation.

$$OH^{\bullet}_{ads} + OH^{\bullet}_{ads} \rightarrow H_2O_2 \quad (12)$$

$$2H_2O + 2h^{+}_{VB} \rightarrow H_2O_2 + 2H^{+} \quad (13)$$

Additional information presented in Fig. 6 indicates that in the case of one and two TiO_2 coatings, there is approximately 50% more peroxide production with internal than with external illumination. In the case of five TiO_2 coatings however, the radiation feeding mode has no effect on the quantity of H_2O_2 generated since in both cases the concentration of H_2O_2 in solution is approximately 6 mg L^{-1}. The production of H_2O_2 on the other hand, decreases for both internal and external illumination when the number of deposits is more than six. This observation is likely due to the loss of TiO_2 film caused by a poor adherence of thick films of

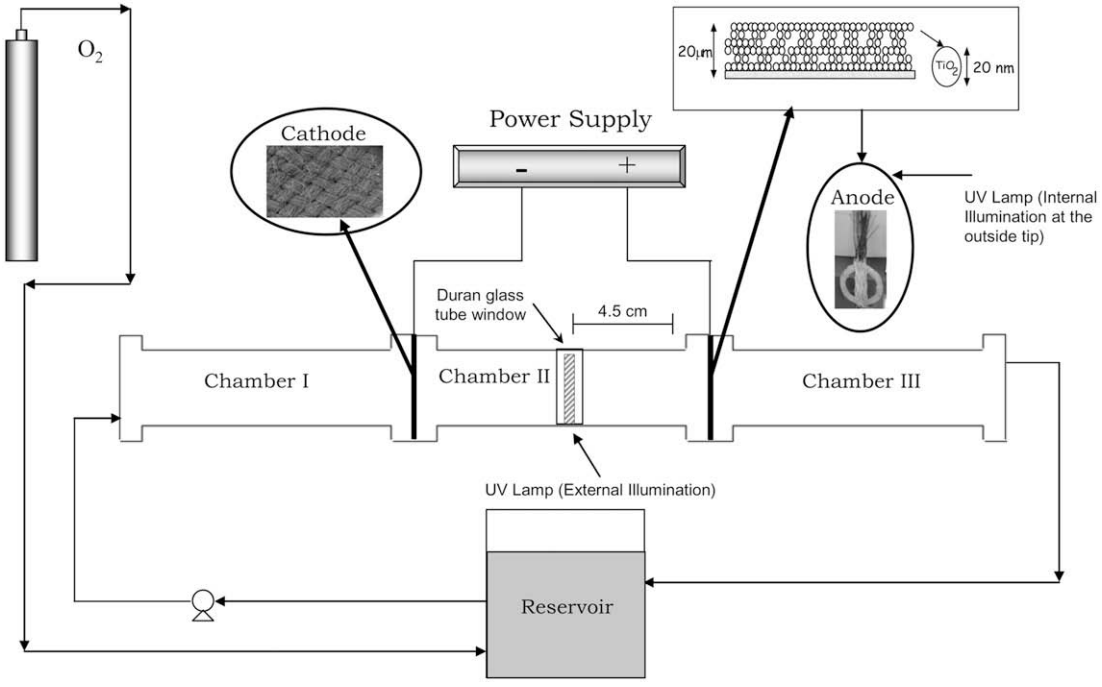

Fig. 7 – Photoelectrochemical reactor scheme. As cathode is used carbon cloth and as anode the TiO_2/modified optical fiber electrode. UV lamp $\lambda = 254$ nm, $P = 21$ W cm^{-2} in both illumination configuration. Reactor volume 640 mL and flow rate 80 L h^{-1}.

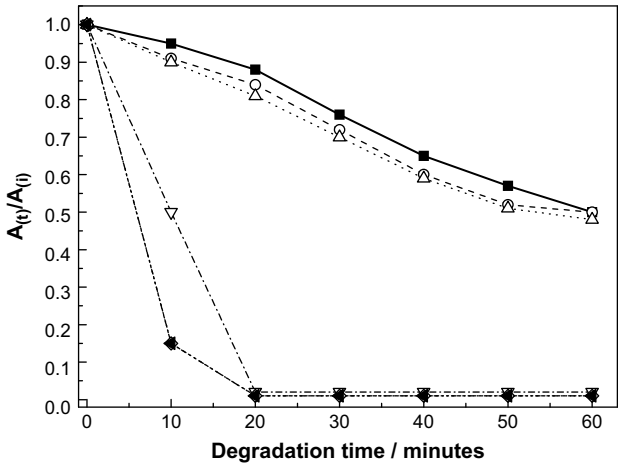

Fig. 8 – Color removal data for Azo orange II dye by different EAOPs. [OG II] 15 mg L^{-1}. Electrolyte 0.05 M Na_2SO_4 solution pH 3. 0.2 mM Fe^{2+} in the Fenton processes. Degradation time 60 min. [H_2O_2] 80 mg L^{-1}. UV lamp $\lambda = 254$ nm, $P = 21$ W cm^{-2} in both illumination configurations. $j = 1$ mA cm^{-2}. Anodic electrooxidation (-■-), Electro-assisted photocatalytic oxidation (external (-○-) and internal illumination (-△-)), electro-Fenton (-▽-), electro-Fenton photoelectrocatalytic Oxidation (external (-◇-) and internal illumination (-◄-)).

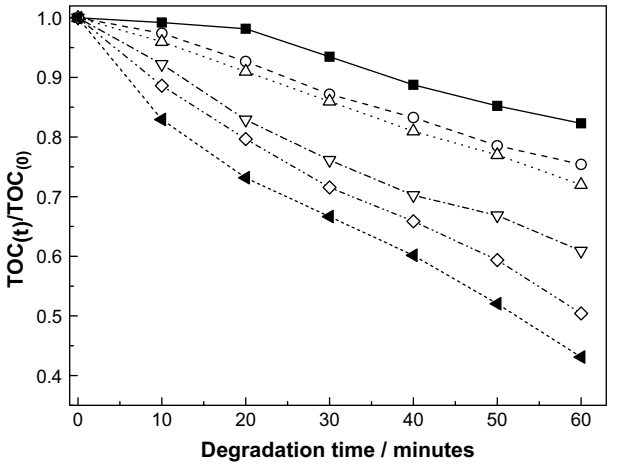

Fig. 9 – Total Organic Carbon removal data for Azo orange II dye by different EAOPs. [OG II] 15 mg L^{-1}. Electrolyte 0.05 M Na_2SO_4 solution pH 3. 0.2 mM Fe^{2+} in the Fenton processes. Degradation time 60 min. [H_2O_2] 80 mg L^{-1}. UV lamp $\lambda = 254$ nm, $P = 21$ W cm^{-2} in both illumination configuration. $j = 1$ mA cm^{-2}. Anodic electrooxidation (-■-), Electro-assisted photocatalytic oxidation (external (-○-) and internal illumination (-△-)), electro-Fenton (-▽-), electro-Fenton photoelectrocatalytic Oxidation (external (-◇-) and internal illumination (-◄-)).

the material. In the case of internal illumination, the decrease of hydrogen peroxide production can also be influenced by charge carrier recombination across the TiO_2 layer.

3.5. *Electrochemical advanced oxidation processes (EAOPs)*

So far, it has been shown that the novel optical fiber supported TiO_2 film has photocatalytic activity for H_2O_2 production and that the internal illumination mode suggested in Fig. 1 works just as well as the external mode of illumination. To verify however that the modified optic fiber could also be polarized and used as a photoanode in an EAOPs, the removal of color and the TOC of a model pollutant compound (azo Dye Orange II) were evaluated using a photoelectrochemical reactor (see Fig. 7) that, as described in the experimental part, incorporated a carbon based cathode and a TiO_2 modified optical fiber-based electrode as an anode. The electrodes in this reactor were polarized three hours before the addition of the dye to assure a suitable concentration of H_2O_2 (the H_2O_2 was electro-generated on the cathode by oxygen reduction and by water oxidation on the anode, see Eqs. (2) and (13) and Section 2.6). In all cases, after 180 min of polarization, the hydrogen peroxide concentration reached approximately 80 mg L^{-1}.

The removal of color in the different electrochemical advanced oxidation processes studied is shown on Fig. 8. The relationship $A_{(t)}/A_{(i)}$ corresponds to the ratio of the absorbance of the solution at 487 nm at the time t, $A_{(t)}$, and at the beginning of the process $A_{(i)}$. The decrease of this ratio is related to the discoloration of the solution. As can be seen from this data, it is possible to remove nearly 50% of the color in the case of the Anodic electrooxidation process. In the Electro-assisted photocatalytic oxidation the color removal is similar to the previous treatment using either internal or external illumination. The similarity between the results using the two illumination configuration modes, also suggest that the photo-induced decomposition of H_2O_2 by UV radiation in solution does not play an important role in the process. On the other hand, when the iron salt in form of Fe^{2+} is added to the reactor (electro-Fenton and electro-Fenton photoelectrocatalytic Oxidation), it is possible to achieve a color removal above 98% due to the rapid concentration increase of the $OH^{\bullet}$ species in solution (Peralta-Hernández et al., 2007, 2008; Abdelmalek et al., 2008). At this point, it is important to note that although the electrochemical or photoelectrochemical regeneration of Fe^{2+} from Fe^{3+} is not possible at the positive charged anode, however the reduction is possible at the negatively polarized cathode surface because, as can be seen in Fig. 7, the iron containing solution is continuously passing through the two electrodes during the process. In addition, reduction also takes place in solution due to the UV light (see Eq. (4)) that, in the case of the internal illumination mode, goes through the SnO_2:Sb and TiO_2 modified optical fiber. Note for instance that, as has been previously described, 50% of the incident light is not absorbed by the SnO_2:Sb and TiO_2 layers (See Sections 2.4 and 3.3 and Fig. 5).

In terms of color removal rates (calculated from the a simple linear correlation employing the first two points of the experimental response for each system), Anodic electrooxidation shows a value ($k = 0.0122$ min^{-1}) that is very similar to that obtained for the Electro-assisted photocatalytic oxidation process when the external illumination arrangement is used ($k = 0.0126$ min^{-1}) and slightly lower to that

computed when the reactor was operated under internal illumination conditions ($k = 0.0131\ min^{-1}$). The electro-Fenton process on the other hand, shows a color removal rate substantially higher ($k = 0.1956\ min^{-1}$) that, as expected, is lower than that obtained if UV light is incorporated into the reaction system. In this case, (electro-Fenton photoelectrocatalytic Oxidation process) the color removal rate ($k = 0.2303\ min^{-1}$) was the same for the two illumination arrangements surveyed.

The results of TOC removal on the other hand, are shown in Fig. 9. Inspection of the curves indicates that when the electro-Fenton photoelectrocatalytic Oxidation process is used, it is possible to achieve a relatively high partial mineralization of the Orange II compound. In this way, using internal illumination (see Fig. 1) it is possible to reach TOC removal values of 57% after 60 min of treatment ($TOC_{(0)}$ value 12.3 ppm and $TOC_{(f)}$ value 5.3 ppm). The lowest percentage of TOC removal on the other hand (of only 15%) was obtained with the Anodic electrooxidation approach. In terms of TOC removal rates (calculated from a simple linear correlation employing the first two points of the experimental response for each system), the electro-Fenton photoelectrocatalytic Oxidation process shows similar k values (0.013 and $0.0109\ min^{-1}$) for the internal and external illumination arrangements. As expected, these constants are higher than those measured for the Electro-assisted photocatalytic oxidation process for which it is also interesting to note that a similar value was found for external and internal illumination modes ($k = 0.0049$ and $0.0055\ min^{-1}$). The lowest k value corresponds to the Anodic electrooxidation ($k = 0.0035\ min^{-1}$). Despite the relatively low percentages of TOC removal found, it is possible to predict better results using longer degradation times.

4. Conclusions

This work has shown that optical fibers previously treated with HF, SnO_2:Sb and electrochemically covered with TiO_2 films can be used as internally illuminated photo anodes to produce $OH^{\bullet}$ radicals in the presence of Fe^{2+} ions. Although an exploratory study, these results are of relevance because the proposed approach can improve the light illumination efficiency in photoelectrochemical reactors; particularly in those designed for water treatment processes. The photoelectrochemical reactor considered in this study is for instance capable of removing 98 % of the color of Azo orange II dye and 57% of TOC in the presence of iron (II) ions using an internal illumination arrangement.

Acknowledgments

The authors thank the Mexican Council for Science and Technology (CONACyT) and the Council for Science and Technology of Guanajuato (CONCyTEG) for financial support of this work (Grant GTO-04-C02-68). They also thank Dr. J.M. Peralta-Hernández for valuable comments and suggestions. K.E.E. also acknowledges CONACyT for a graduate fellowship.

REFERENCES

Abdelmalek, F., Torres, R.A., Combet, E., Petrier, C., Pulgarin, C., Addou, A., 2008. Gliding arc discharge (GAD) assisted catalytic degradation of bisphenol A in solution with ferrous ions. Separation and Purification Technology. doi:10.1016/j.seppur.2008.03.036.

Bandala, Erick R., Peláez, Miguel A., Garcìa-López, A., Salgado, Maria de J., Moeller, Gabriela, 2008. Photocatalytic decolourisation of synthetic and real textile wastewater containing benzidine-based azo dyes. Chemical Engineering and Processing 47, 169–176.

Bandara, J., Wansapura, P.T., Jayathilaka, S.P.B., 2007. Indium tin oxide coated conducting glass electrode for electrochemical destruction of textile colorants. Electrochimica Acta 52, 4161–4166.

Bauer, R., Waldner, G., Fallmann, H., Hager, S., Klare, M., Krutzler, T., Malato, S., Maletzky, P., 1999. The photo-Fenton reaction and the TiO_2/UV process for waste water treatment-novel developments. Catalysis Today 53, 131–144.

Boye, B., Dieng, M.M., Brillas, E., 2002. Degradation of herbicide 4-chlorophenoxyacetic acid by advanced electrochemical oxidation methods. Environmental Science Technology 36, 3030–3035.

Boye, B., Mariéme Dieng, M., Brillas, E., 2003. Electrochemical degradation of 2,4,5-trichlorophenoxyacetic acid in aqueous medium by peroxi-coagulation: effect of pH and UV light. Electrochimica Acta 48, 781–790.

Brillas, E., Baños, M.A., Garrido, J.A., 2003. Mineralization of herbicide 3,6-dichloro-2-methoxybenzoic acid in aqueous medium by anodic, electro-Fenton and photoelectro-Fenton. Electrochimica Acta 48, 1697–1705.

Choi, Wonyong, Ko, Joung Yun, Park, Hyunwoonh, Chung, Jong Shik, 2001. Investigation on TiO_2-coated optical fibers for gas-phase photocatalytic oxidation of acetone. Applied Catalysis B: Environmental 31, 209–220.

Danion, Anne, Bordes, Calire, Disdier, Jean, Gauvrit, Jean Yves, Guillard, Chantal, Lantéri, Pierre, Jaffrezic-Renault, Nicole, 2004a. Optimization of a single TiO_2-coated optical fiber reactor using experimental design. Journal of Photochemistry and Photobiology A: Chemistry 168, 161–167.

Danion, Anne, Disdier, Jean, Guillard, Chantal, Abdelmalek, Fethi, Jaffrezic-Renault, Nicole, 2004b. Characterization and study of a single-TiO_2-coated optical fiber reactor. Applied Catalysis B: Environmental 52, 213–223.

Danion, Anne, Disdier, Jean, Guillard, Chantal, Païssé, Oliver, Jaffrezic-Renault, Nicole, 2006. Photocatalytic degradation of imidazolinone fungicide in TiO_2-coated optical fiber reactor. Applied Catalysis B: Environmental 62, 274–281.

Danion, Anne, Disdier, Jean, Guillard, Chantal, Jaffrezic-Renault, Nicole, 2007. Malic acid photocatalytic degradation using a TiO_2-coated optical fiber reactor. Journal of Photochemistry and Photobiology A: Chemistry 190, 135–140.

Elangovan, E., Ramamurthi, K., 2003. Effect of substrate temperature on electrical and optical properties of spray deposited SnO_2:Sb thin films. Journal of Optoelectronics and Advanced Materials 5-2, 415–420.

Flox, Cristina, Cabot, Pere Lluís, Centellas, Francesc, Garrido, José Antonio, Rodríguez, Rosa María, Arias, Conchita, Brillas, Enric, 2007a. Solar photoelectro-Fenton degradation of cresols using a flow reactor with a boron-doped diamond anode. Applied Catalysis B: Environmental 75, 17–28.

Flox, C., Garrido, J.A., Rodríguez, R.M., Cabot, P.L., Centellas, F., Arias, C., Brillas, E., 2007b. Mineralization of herbicide mecoprop by photoelectro-Fenton with UVA and solar light. Catalysis Today 129, 29–36.

Fujishima, A., Rao, T.N., Donal, T.A., 2000. Titanium dioxide photocatalysis. Journal of Photochemistry and Photobiology C: Photochemical Review 1, 1–21.

Gianluca, Li Puma, Bono, Awang, Krishnaianh, Duduku, Collin, Joseph G., 2008. Preparation of titanium dioxide photocatalyst loaded onto activated carbon support using chemical vapor deposition: a review paper. Journal of Hazardous Materials 157, 209–219.

Guinea, Elena, Arias, Conchita, Cabot, Pere Lluís, Garrido, José Antonio, Rodríguez, Rosa María, Centellas, Francesc, Brillas, Enric, 2008. Mineralization of salicylic acid in acidic aqueous medium by electrochemical advanced oxidation processes using platinum and boron-doped diamond as anode and cathodically generated hydrogen peroxide. Water Research 42, 499–511.

Gumy, D., Giraldo, S.A., Rengifo, J., Pulgarin, C., 2008. Effect of suspended TiO_2 physicochemical characteristics on benzene derivatives photocatalytic degradation. Applied Catalysis B: Environmental 78, 19–29.

Hou, Yining, Qu, Juihui, Zhao, Xu, Lei, Pengju, Wan, Dongjin, Huang, C.P., 2009. Electro-photocatalytic degradation of acid orange II using a novel TiO_2/ACF photoanode. Science of the Total Environment 407 (7), 2431–2439.

Jiang, Dianlu, Zhao, Huijun, Zhang, Shanqing, John, Richard, 2006. Comparison of photocatalytic degradation kinetic characteristics of different organic compounds at anatase TiO_2 nanoporous film electrodes. Journal of Photochemistry and Photobiology A: Chemistry 177, 253–260.

Lapertot, Milena, Ebrahimi, Sirous, Oller, Isabel, Maldonado, Manuel I., Gernjak, Wolfgang, Malato, Sixto, Pulgarín, César, 2008. Evaluating Microtox® as a tool for biodegradability assessment of partially treated solutions of pesticides using Fe^{3+} and TiO_2 solar photo-assisted processes. Ecotoxicology and Environmental Safety 69, 546–555.

Li, Guoting, Qu, Jiuhui, Zhang, Xiwang, Ge, Jiantuan, 2006. Electrochemically assisted photocatalytic degradation of acid orange 7 with b-PbO_2 electrodes modified by TiO_2. Water Research 40, 213–220.

Lou, Jie-Chung, Huang, Yu-Jen, 2008. Assessing the performance of wastewater treatment with the combination of Fenton and ferrite process. Environmental Monitoring Assessment. doi:10.1007/s10661-008-0266-x.

Manriquez, J., Godínez, Luis A., 2007. Tuning the structural, electrical and optical properties of Ti(III)-doped nanocrystalline TiO_2 films by electrophoretic deposition time. Thin Solid Films 515, 3402–3413.

Marinangeli, Richard E., Ollis, David F., 1977. Photo-assited heterogeneous catalysis with optical fibers. AlChE 23-4, 415–426.

Marinangeli, Richard E., Ollis, David F., 1980. Photo-assited heterogeneous catalysis with optical fibers, II. Nonisothermal single fiber and fiber bundle. AlChE 26-6, 1000–1008.

Marinangeli, Richard E., Ollis, David F., 1982. Photo-assited heterogeneous catalysis with optical fibers, III. Photoelectrodes. AlChE 28-6, 945–955.

Martínez-Huitle, Carlos A., Brillas, Enric, 2009. Decontamination of wastewaters containing synthetic organic dyes by electrochemical methods: a general review. Applied Catalysis B: Environmental 87 (3–4, 7), 105–145.

Miller, Lawrence W., Tejedor-Tejedor, Isabel, Anderson, Marc A., 1999. Titanium dioxide-coated silica waveguides for the photocatalytic oxidation of formic acid in water. Environmental Science Technology 33, 2070–2075.

Neelavannan, M.G., Ahmed Basha, C., 2008. Electrochemical-assisted photocatalytic degradation of textile washwater. Separation and Purification Technology 61 (2), 168–174.

Orozco, Sayra L., Bandala, Erick R., Arancibia-Bulnes, Camilo A., Serrano, Benito, Suárez-Parra, Raúl, Hernández-Pérez, Isaias, 2008. Effect of iron salt on the color removal of water containing the azo-dye reactive blue 69 using photo-assisted Fe(II)/H_2O_2 and Fe(III)/H_2O_2 systems. Journal of Photochemistry and Photobiology A: Chemistry 198, 144–149.

Oturan, Nihal, Trajkovska, Snezana, Oturan, Mehmet A., Couderchet, Michel, Aaron, Jean-Jacques, 2008. Study of the toxicity of diuron and its metabolites formed in aqueous medium during application of the electrochemical advanced oxidation process ''electro-Fenton''. Chemosphere 73 (9), 1550–1556.

Özcan, Ali, Oturan, Mehmet A., Oturan, Nihal, Şahin, Yücel, 2009. Removal of acid orange 7 from water by electrochemically generated Fenton's reagent. Journal of Hazardous Materials 163 (2–3), 213–1220.

Pallas, Ramon, 2005. Sensors and Signal Conditioners, fourth ed. Marcombo Publishing, ISBN 8426713440 (Chapter 2).

Peill, Nicola J., Hoffmann, Michael R., 1995. Development and optimization of a TiO_2-coated fiber-optic cable reactor: photocatalytic degradation of 4-cholophenol. Environmental Science Technology 29, 2974–2981.

Peill, Nicola J., Hoffmann, Michael R., 1998. Mathematical model of a photocatalytic fober-optic cable reactor for heterogeneous photocatalysis. Environmental Science Technology 32, 398–404.

Peralta-Hernández, J.M., Meas-Vong, Yunny, Rodriguez, Francisco J., Chapman, Thomas W., Maldonado, Manuel I., Godínez, Luis A., 2006. In situ electrochemical and photo-electrochemical generation of the Fenton reagent: a potentially important new water treatment technology. Water Research 40, 1754–1762.

Peralta-Hernández, J.M., Manriquez, J., Meas-Vong, Y., Rodriguez, Francisco J., Chapman, Thomas W., Maldonado, Manuel I., Godínez, Luis A., 2007. Photocatalytic properties of nano-structured TiO_2-carbon films obtained by means of electrophoretic deposition. Journal of Hazardous Materials 147, 588–593.

Peralta-Hernández, J.M., Meas-Vong, Yunny, Rodriguez, Francisco J., Chapman, Thomas W., Maldonado, Manuel I., Godínez, Luis A., 2008. Comparison of hydrogen peroxide-based processes for treating dye-containing wastewater: decolorization and destruction of orange II azo dye in dilute solution. Dyes and Pigments 76, 656–662.

Russo, B., Cao, G.Z., 2008. Fabrication and characterization of fluorine-doped thin oxide films and nanorod arrays via spray pyrolysis. Applied Physics A 90, 311–315.

Selcuk, H., Zaltner, W., Sene, J.J., Bekbolet, M., Anderson, M.A., 2004. Photocatalytic and photoelectrocatalytic performance of 1% Pt doped TiO_2 for the detoxification of water. Journal of Applied Electrochemistry 34, 653–658.

Serra, Anna, Domènech, Xavier, Arias, Conchita, Brillas, Enric, Peral, José., 2008. Oxidation of α-methylphenylglycine under Fenton and electro-Fenton conditions in the dark and in the presence of solar light. Applied Catalysis B: Environmental. doi:10.1016/j.apcatb.2008.11.022.

Sirés, I., Garrido, J.A., Rodríguez, R.M., Cabot, P.L., Centellas, F., Arias, C., Brillas, E., 2006. Electrochemical degradation of paracetamol from water by catalytic action of Fe^{2+}, Cu^{2+} and UVA light on electrogenerated hydrogen peroxide. Journal of Electrochemical Society 153 (1), D1–D9.

Skoumal, Marcel, Rodríguez, Rosa María, Cabot, Pere Lluís, Centellas, Francesc, Garrido, José Antonio, Arias, Conchita, Brillas, Enric, 2009. Electro-Fenton, UVA photoelectro-Fenton and solar photoelectro-Fenton degradation of the drug ibuprofen in acid aqueous medium using platinum and boron-doped diamond anodes. Electrochimica Acta 54 (7), 2077–2085.

Tomovska, Radmila, Marinkovski, Mirko, Frajgar, Radek, 2007. Current state of nanostructured TiO_2-based catalysts: preparation methods. Nanotechnology – Toxicological Issues and Environmental Safety, 207–229.

Virkutyte, Jurate, Jegatheesan, Veeriah, 2009. Electro-Fenton, hydrogenotrophic and Fe^{2+} ions mediated TOC and nitrate removal from aquaculture system: different experimental strategies. Bioresource Technology 100 (7), 2189–2197.

Wang, Chen, Li, Jun, Mele, Giuseppe, Yang, Gao-Mai, Zhang, Feng-Xing, Palmisano, Leonardo, Vasapollo, Giuseppe, 2007. Efficient degradation of 4-nitrophenol by using functionalized porphyrin-TiO2 photocatalysts under visible irradiation. Applied Catalysis B: Environmental 76, 218–226.

Wang, Jiade, Mei, Yu, Liu, Chenliang, Chen, Jianmeng, 2008. Chlorobenzene degradation by electro-heterogeneous catalysis in aqueous solution: intermediates and reaction mechanism. Journal of Environmental Sciences 20 (11), 1306–1311.

Wang, Weng, Ku, Young, 2003. The light transmission and distribution in an optical fiber coated with TiO_2 particles. Chemosphere 59, 999–1006.

Wang, Ya-qiong, Gu, Bin, Xu, Wen-lin, 2009. Electro-catalytic degradation of phenol on several metal-oxide anodes. Journal of Hazardous Materials 162 (2–3), 1159–1164.

Xie, Y.B., Li, X.Z., 2006. Interactive oxidation of photoelectrocatalysis and electro-Fenton for azo dye degradation using TiO_2–Ti mesh and reticulated vitreous carbon electrodes. Materials Chemistry and Physics 95, 39–50.

Yang, Xiupei, Zou, Ruyi, Huo, Feng, Cai, Duochang, Xiao, Dan, 2009. Preparation and characterization of Ti/SnO_2–Sb_2O_3–Nb_2O_5/PbO_2 thin film as electrode material for the degradation of phenol. Journal of Hazardous Materials 164 (1), 367–373.

Yu, BinBin, Zeng, JingBin, Gong, LiFen, Yang, XiaoQing, Zhang, LiMei, Chen, Xi, 2008. Photocatalytic degradation investigation of dicofol. Chinese Science Bulletin 53 (1), 27–32.

Zhao, Huijun, Jiang, Dianlu, Zhang, Shanqing, Wen, William, 2007. Photoelectrocatalytic oxidation of organic compounds at nanoporous TiO_2 electrodes in a thin-layer photoelectrochemical cell. Journal of Catalysis 250, 102–109.